Circulation: Heart Failure

ADVANCES IN HEART FAILURE

Invasive Right Ventricular Pressure-Volume Analysis: Basic Principles, Clinical Applications, and Practical Recommendations

Michael I. Brener, MD; Amirali Masoumi, MD; Vivian G. Ng, MD; Khodr Tello, MD; Marcelo B. Bastos, MD; William K. Cornwell III, MD, MSCS; Steven Hsu, MD; Ryan J. Tedford, MD; Philipp Lurz, MD, PhD; Karl-Philipp Rommel, MD; Karl-Patrik Kresoja, MD; Sherif F. Nagueh, MD; Manreet K. Kanwar, MD; Navin K. Kapur, MD; Gurumurthy Hiremath, MD; Mohammad Sarraf, MD; Antoon J.M. Van Den Enden, MD; Nicolas M. Van Mieghem, MD, PhD; Paul M. Heerdt, MD, PhD; Rebecca T. Hahn, MD; Susheel K. Kodali, MD; Gabriel T. Sayer, MD; Nir Uriel, MD, MS; Daniel Burkhoff, MD, PhD

ABSTRACT: Right ventricular pressure-volume (PV) analysis characterizes ventricular systolic and diastolic properties independent of loading conditions like volume status and afterload. While long-considered the gold-standard method for quantifying myocardial chamber performance, it was traditionally only performed in highly specialized research settings. With recent advances in catheter technology and more sophisticated approaches to analyze PV data, it is now more commonly used in a variety of clinical and research settings. Herein, we review the basic techniques for PV loop measurement, analysis, and interpretation with the aim of providing readers with a deeper understanding of the strengths and limitations of PV analysis. In the second half of the review, we detail key scenarios in which right ventricular PV analysis has influenced our understanding of clinically relevant topics and where the technique can be applied to resolve additional areas of uncertainty. All told, PV analysis has an important role in advancing our understanding of right ventricular physiology and its contribution to cardiovascular function in health and disease.

Key Words: heart failure ■ hemodynamics ■ pulmonary circulation ■ ventricular function, right

Right ventricular (RV) function is a major determinant of morbidity and mortality for a variety of cardiovascular diseases.[1] Despite its importance, RV function is challenging to characterize and quantify. Two-dimensional imaging modalities like echocardiography struggle to negotiate the ventricle's irregular position in the chest and its asymmetrical geometry. As a result, 2-dimensional-based echocardiographic measurements like tricuspid annular systolic plane excursion and RV free wall longitudinal strain only characterize contractile function in a single direction or from a particular aspect of the ventricle. More sophisticated modalities like cardiac magnetic resonance (CMR) and 3-dimensional echocardiographic imaging, while able to overcome some of these limitations, provide predominantly volume-centric descriptions of RV function. Invasive assessments like right heart catheterization (RHC) are also limited in that they provide a pressure-centric perspective of RV function. Furthermore, all of these metrics of RV function—whether derived from imaging modalities or RHC—are subject to the influence of loading conditions.

Pressure-volume (PV) analysis addresses these shortcomings by combining simultaneous measurements of pressure and volume to generate load-independent measures of systolic and diastolic chamber properties, and is considered the gold-standard method for characterizing ventricular systolic and diastolic function, as well as ventricular-vascular interactions (Figure 1).[2] Moreover,

Correspondence to: Michael I. Brener, MD, Division of Cardiology, Columbia University Medical Center, Presbyterian Hospital, 622 W 168th St, 3rd Floor, Room 347, New York, NY 10087. Email mib2102@cumc.columbia.edu

This manuscript was sent to Prof. Walter J. Paulus, MD, PhD, Guest Editor, for review by expert referees, editorial decision, and final disposition.
Supplemental Material is available at https://www.ahajournals.org/doi/suppl/10.1161/CIRCHEARTFAILURE.121.009101.
For Sources of Funding and Disclosures, see page 99.

Circulation: Heart Failure is available at www.ahajournals.org/journal/circheartfailure

Nonstandard Abbreviations and Acronyms

C_{ed}	end-diastolic volume measurements from the conductance catheter
C_{es}	end-systolic volume measurements from the conductance catheter
CMR	cardiac magnetic resonance
E_a	effective arterial elastance
EDPVR	end-diastolic PV relationship
E_{es}	end-systolic elastance
EF	ejection fraction
ESPVR	end-systolic PV relationship
HF	heart failure
HFpEF	heart failure with preserved ejection fraction
LV	left ventricle
LVAD	LV assist device
PA	pulmonary artery
PAH	pulmonary arterial hypertension
P_{es}	end-systolic pressure
PV	pressure-volume
RHC	right heart catheterization
RV	right ventricle
SV	stroke volume
TR	tricuspid regurgitation
V_{ed}	end-diastolic ventricular volume

it is able to capture the dynamic changes in these relationships throughout the cardiac cycle in a way that pump function curves, which relate mean ventricular pressure to stroke volume (SV), cannot.[3] Recent advances in catheter technology and analysis of PV data have made the technique more accessible and easier to perform. While these techniques have been widely applied to understanding left ventricular (LV) mechanics in health and disease, they have only recently been applied in the RV with greater frequency. Herein, we review the basic principles underlying RV PV analysis, as well as appropriate clinical and research-related applications that can advance our understanding of RV function and RV-pulmonary artery (PA) interactions.

METHODS USED TO MEASURE RV PV LOOPS

PV analysis is performed with a specialized high-fidelity conductance catheter. While multiple catheter designs exist, currently, only CD Leycom (Hengelo, the Netherlands) manufactures a conductance catheter for clinical PV analysis that can be used in either the RV or LV. The principles of operation have been detailed previously[4] and are illustrated in Figure 2. The catheter terminates with a pig-tail loop. Two sizes are produced: a 7F version that is inserted over a wire via Seldinger technique and a 4F version without a lumen. The catheter features a solid-state pressure sensor in the middle of an array of twelve equally spaced electrodes at its tip (3 versions of the conductance catheter are produced with electrodes spaced either 8, 10, or 12 mm apart). A high frequency alternating electrical current of known amplitude passing between the most proximal and most distal electrodes sets up an electric field within the RV. Voltage drops measured between successive pairs of electrodes are inversely proportional to the cross-sectional RV area at the level of each electrode; segmental volumes are estimated by the product of that cross-sectional area and the known, fixed distance between electrodes. Total ventricular volume is then calculated by summation of the segmental volumes of each electrode pair resting within the RV chamber.

RV PV LOOP MEASUREMENT TECHNIQUE

RV PV loop measurements are traditionally obtained from either a right internal jugular or common femoral venous approach, depending on investigator preference. Maneuvering the conductance catheter into the RV apex from a femoral approach may be challenging under certain circumstances, but a frontrunning wire loop in the right atrium, a long sheath, and use of a steerable sheath can help overcome most difficulties.[5] The 7F catheter is generally preferred because the over-the-wire technique maximizes the chances of successfully manipulating the catheter into the RV apex. Unique scenarios, for example, patients with LV assist devices (LVADs) on anticoagulation, may warrant use of the smaller 4F catheter. Insertion of a sheath that is at least 1F size larger than the conductance catheter allows operators to use the sheath's side port for blood draws and infusions. While a standard exchange-length 0.025-inch J-tipped guidewire usually suffices for routine insertion, escalation to a stiffer guidewire (ie, Platinum Plus 0.025-inch guidewire, Boston Scientific, Marlborough, MA) may be necessary to facilitate appropriate placement of the catheter. All catheter manipulations should be performed under fluoroscopic guidance, and studies in patients with a recently implanted pacemaker or defibrillator lead should be avoided.

PV loops should be analyzed at end expiration to minimize the contribution of intrathoracic pressure to RV pressure measurements (Figure S1). Accordingly, it is important to record clips that include a minimum of 2 respiratory cycles to be able to clearly identify loops at end expiration. For patients who are intubated, PV loops may be acquired during a breath-hold maneuver to minimize variance in hemodynamics that occur throughout the respiratory cycle. Furthermore, data segments should be free of extra-systoles or other arrhythmias since

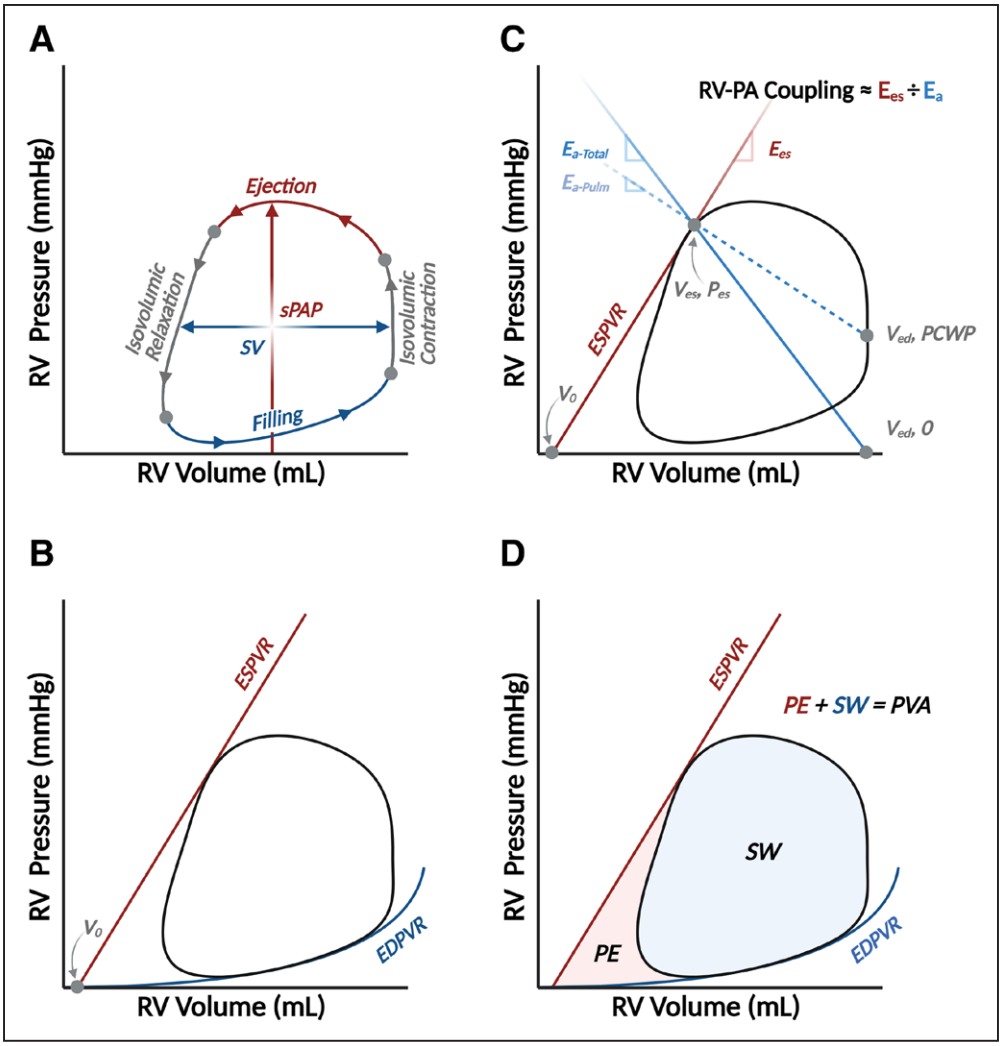

Figure 1. Basic elements of the right ventricular (RV) pressure-volume (PV) diagram.
The PV diagram summarizes hemodynamic changes during 1 cardiac cycle, which is divided into 4 phases: ventricular filling, isovolumic contraction, ejection, and isovolumic relaxation (**A**). The width of the loop represents ventricular stroke volume (SV), and the peak pressure is RV or pulmonary artery systolic pressure (sPAP). Two fundamental relationships create boundaries for the PV loop: the end-systolic PV relationship, which describes ventricular contractile properties, and the end-diastolic PV relationship (EDPVR), which describes ventricular diastolic function (**B**). End-systolic PV relationship (ESPVR) is reasonably linear and connects the ESPV coordinate with the volume-axis intercept (V_0) or the unstressed blood volume of the ventricle. The PV loop is also a valuable platform to relate vascular properties. Afterload can be characterized by effective arterial elastance, which is a lumped parameter ($E_{a\text{-}Total}$) reflecting the influence of downstream pressure (ie, pulmonary capillary wedge pressure, PCWP) and intrinsic properties of the pulmonary vasculature ($E_{a\text{-}Pulm}$). $E_{a\text{-}Pulm}$ is reflected by the slope of the line connecting the ESPV coordinate with (V_{ed}, PCWP), while $E_{a\text{-}Total}$ connects the end-systolic coordinates and the V_0 at end-diastolic volume (V_{ed}, 0).[2] Relating systolic function, summarized by the slope of ESPVR (also known as end-systolic elastance, E_{es}), to E_a is the foundation of a concept called RV-pulmonary arterial (PA) coupling (**C**). Finally, myocardial energetics can also be inferred from the PV diagram. The space within the loop is stroke work (SW), and the potential space bound within the ESPVR and EDPVR but outside the loop is the potential energy (PE). The sum of SW and PE is PV area (PVA), which is linearly related to myocardial oxygen consumption (**D**).

they are not representative of the chamber's mechanical state and may interfere with interpretation of the PV loop.[6] The conductance catheter must be occasionally retracted off the RV wall to quell arrhythmias. In patients with atrial fibrillation, beats with similar R-R intervals are preferred for analysis. Finally, it should be noted that the conductance catheter may tether the tricuspid valve and introduce tricuspid regurgitation (TR), especially when additional catheters (ie, Swan-Ganz catheter) are also crossing the valve. This phenomenon can be detected on the PV loop by exaggerated volume loss during the isovolumetric relaxation phase and can be resolved by either manipulating the catheter or attempting an alternative approach to enter the RV (ie, switch from femoral to internal jugular venous access).

CONDUCTION CATHETER CALIBRATION

The raw time varying signal provided by the conductance catheter, that is, the conductance signal, C(*t*), is

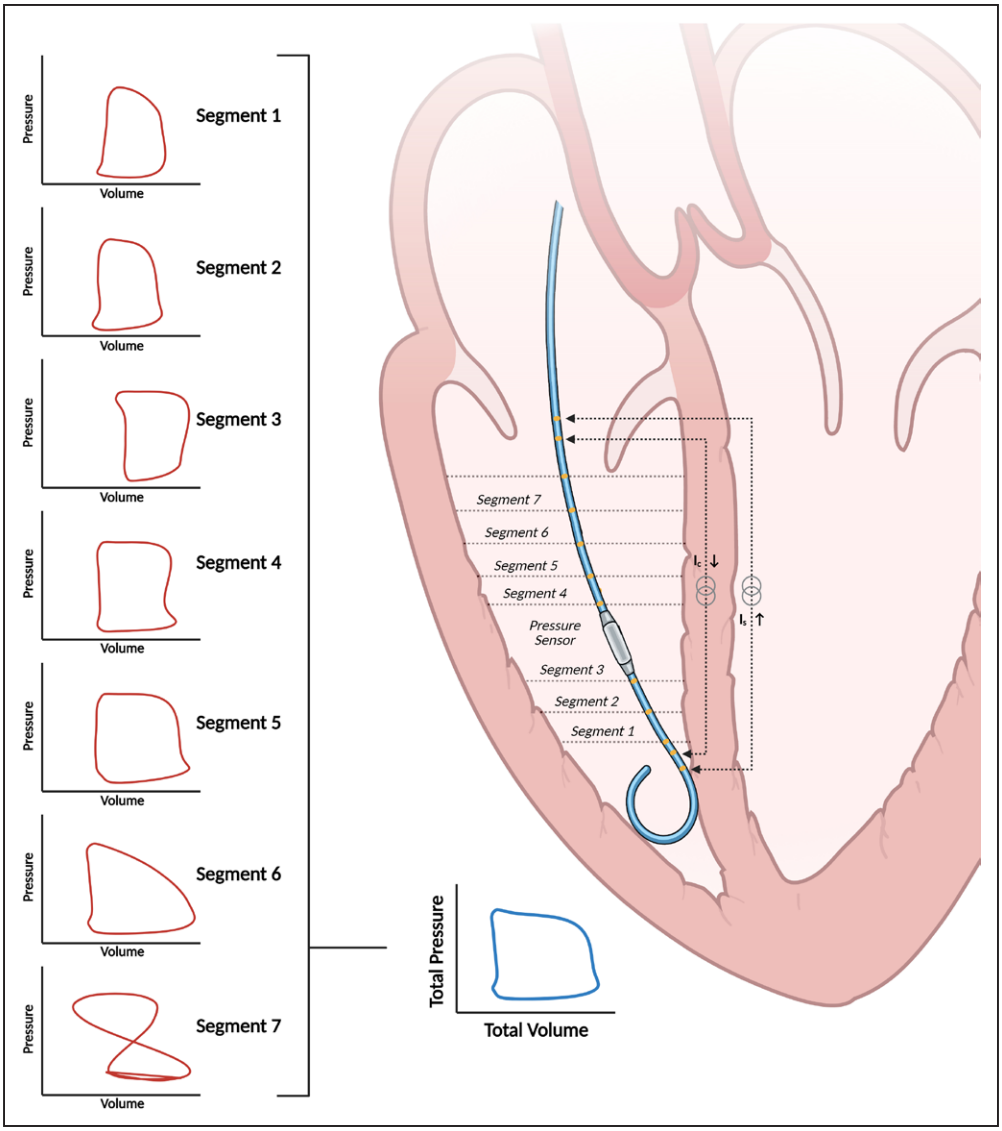

Figure 2. Conductance volumetry for pressure-volume analysis in the right ventricle.
The catheter estimates ventricular volumes through the principle of conductance volumetry. Volumes from segments 1 through 6 in this case are used to calculate overall ventricular volume because the loop in segment 7 is not counterclockwise, indicating that the electrode is extraventricular.

proportional to absolute RV volume over time. A gain factor (α) and an offset factor (V_p, called the parallel conductance offset) are required to convert this signal into absolute volume. There are different techniques for obtaining these calibration factors. α is typically calculated by dividing the SV measured from other modalities by the difference between end-systolic and end-diastolic volume measurements from the conductance catheter (C_{ed}–C_{es}) such that α=SV/(C_{ed}–C_{es}).[7] SV is typically determined from RHC (ie, thermodilution or fick determination of cardiac output divided by heart rate) or from an imaging modality. One method for determining V_p involves a rapid, 10 mL intravenous injection of hypertonic saline (5%–10% NaCl) upstream from the conductance catheter (eg, through the sheath side port). Hypertonic saline changes the conductivity of blood and, despite a constant time course of volume change during the cardiac cycle, the recorded C(t) signal increases progressively until returning to baseline as the hypertonic saline is cleared (Figure S2). Baan et al[8] outlined a method where the parallel conductance offset is determined by the intersection between the line of identity with a regression line derived when catheter-derived end-systolic pressure is plotted against end-diastolic pressure.[8] However, the slope of the regression line, and therefore, the location where the regression line intersects with the line of identity, is subject to error when derived from only a few PV loops recorded under the influence of hypertonic saline. These limitations, as well as the implications of administering a salt load in patients with ventricular dysfunction, can be bypassed entirely by an alternative approach to determining V_p, which relies on an imaging modality, typically either CMR (which has the advantage of accurate volumetric assessment) or

3-dimensional echocardiography (which has the advantage of being able to be performed in real-time as the PV loops are recorded) to obtain end-diastolic ventricular volume (V_{ed}). After adjusting the conductance signal by the gain factor, V_p is simply determined by subtraction: $V_p = \alpha \cdot C_{ed} - V_{ed}$. These gain factors are sensitive to conductance catheter position and the number of segments included in the estimation of total RV volume (discussed further below). Accordingly, new values of calibration factors are required each time the conductance catheter is moved and this should be considered when designing experiments where measurements required for repeated calibrations are not feasible.

PV LOOP ANALYSIS

The first step in the analysis involves choosing which of the available 7 segments to include in the determination of total ventricular volume. Recall that the conductance catheter produces segmental PV loops from each adjacent pair of electrodes, and these segmental volumes are summated to produce the overall ventricular volume. However, depending on the size of the RV and the position of the catheter, some segments may not reside in the RV chamber. Segments outside the RV can be readily identified by irregularly shaped segmental loops, especially those which progress over time in a clockwise direction (volume increases during systole) instead of the normal counterclockwise direction (volume decreases during systole; Figure 2). Abnormally shaped segmental loops may also be observed, reflecting contact with the ventricular wall, papillary apparatus, or the moderator band. These segments should be excluded, and it is critical that the same segments are used throughout the analysis of multiple loops measured over time.

Describing ventricular systolic and diastolic properties is among the key objectives of PV analysis, and this can be achieved by characterizing the end-systolic and end-diastolic PV relationships (ESPVR and EDPVR, respectively). The ESPVR is generally considered to be linear and characterized by a slope (end-systolic elastance, E_{es}) and a volume-axis intercept (V_0). The EDPVR is nonlinear and has been characterized by different equations incorporating multiple parameters. These relationships can be assessed in 2 ways. The first method, referred to as the multibeat method, connects ventricular pressure and volume coordinates at end-systole and end-diastole from a family of PV loops recorded under different loading conditions (Figure 3A).[9] This technique is limited by the need to perform maneuvers that alter loading conditions, such as the Valsalva maneuver, external abdominal compression, or balloon occlusion of the inferior vena cava, which may have secondary effects on sympathetic tone and contractile function. For example, the Valsalva maneuver increases sympathetic tone during phase IIB of the maneuver, which may artificially increase ventricular contractility and confound PV measurements. Furthermore, this method and other noninvasive methods like external abdominal compression require substantial patient cooperation and may not be feasible in all circumstances. Balloon occlusion is advantageous since it does not lead to any changes in sympathetic tone and is, therefore, our preferred method. However, balloon occlusion requires additional venous access, which may not be possible in certain clinical scenarios (eg, during surgical procedures and anatomic constraints) or compatible with all protocols (eg, those requiring lower extremity exercise). Finally, while these preload reducing maneuvers allow for accurate characterization of the ESPVR, they do not describe the exponential portion of the EDPVR, which occurs at larger volumes. As such, preload reducing maneuvers perform better at describing the portion of the EDPVR at lower volumes and pressures.

To overcome these technical challenges, single-beat methods for estimating both ESPVR and EDPVR have been described and validated.[10,11] Initially developed for the LV, single-beat estimation of the ESPVR most commonly entails prediction of the maximal pressure that would have been achieved if ventricular contraction remained isovolumic (P_{max}; Figure 3B). Sunagawa et al[12] established a method for fitting an equation to the isovolumic portions of the LV pressure-time curve to derive a value for P_{max}. When combined with end-systolic pressure (P_{es}) and measurement of SV, this method provides an estimate of the slope of the ESPVR expressed as E_{es} in mm Hg/mL and calculated as $(P_{max} - P_{es})/SV$. Brimioulle et al[13] have validated a single-beat estimation of ESPVR using P_{max} from invasive PV data, but extrapolating P_{max} from the more readily available RV pressure-time tracings is more challenging in the RV than in the LV because the beginning and end of the isovolumic periods are less well defined. Accordingly, methods have been described to improve identification of these discrete time points during the cardiac cycle and, thus, provide less variable predictions of P_{max}. For example, taking the second derivative squared of the RV pressure signal identifies 4 peaks that can be used to mark the beginning and end of the isovolumic periods (contraction=EDP to P_i and relaxation=P_{es} to end-systole; Figure 3C). This method has been validated not only under normal conditions, where end-systolic pressure is significantly lower than peak RV pressure when ejection is prolonged, but also when pulmonary hypertension is present, end-systolic pressure and peak RV pressure are similar, and ejection time is shortened, similar to what is observed in the LV (Figure 3D). The challenges associated with this P_{max}-based method can also be obviated with an alternative method for estimating the slope of the ESPVR, which was proposed by Senzaki et al,[14] whereby V_0 is estimated and the ESPVR is determined by the line connecting the end-systolic coordinate (V_{es} and P_{es}) with volume-axis intercept (Figure 3E). While

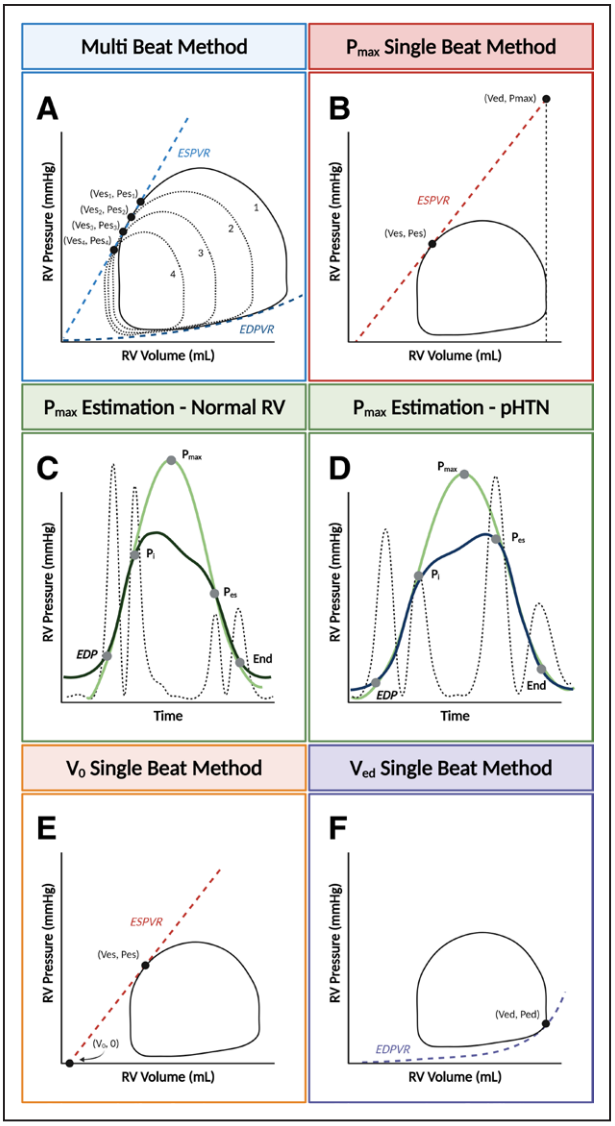

Figure 3. Multi- and single-beat methods and notable limitations for estimating end-systolic pressure-volume relationships (ESPVR).
The ESPVR can be modeled with 2 different methods: the multibeat method (**A**), which plots ESPVR by connecting serial end-systolic PV coordinates, or the single-beat method, which extrapolates either the maximal isovolumic pressure (P_{max}; **B**) or the volume-axis intercept (V_0). P_{max} is represented by the peak of a curve fitted to discrete points during the cardiac cycle from the right ventricular (RV) pressure waveform. Determination of these time points can be standardized by taking the second derivative of RV pressure squared (hatched line). With this method, the up interval for P_{max} prediction extends from end-diastolic pressure (EDP) to the first major inflection point (P_i), and the down interval from end-systolic pressure (P_{es}) to the estimated end of isovolumic relaxation. This method is validated in patients with normal RV pressures (**C**) and pulmonary hypertension (pHTN; **D**). Alternatively, determination of V_0 can be used with the single-beat method (**E**). Finally, the single-beat method for determining the EDPV relationship (EDPVR) relies on the end-diastolic coordinate (V_{ed}, P_{ed}; **F**).

this method has been compared with noninvasively constructed PV loops using CMR and RHC data in patients with pulmonary hypertension,[15] it has not been directly validated against RV PV loops obtained using the conductance method.

Aided by recent efforts to standardize the prediction of P_{max} and definition of P_{es}, simultaneous single-beat estimations of RV E_{es} and effective arterial elastance (E_a) have also become widely used to characterize RV-PA coupling.[16–18] Using these refinements, Richter et al[19] reported that in a clinical population with pulmonary arterial hypertension (PAH), single-beat quantification of RV-PA coupling accurately reflected RV-PA coupling measured using the multibeat method.

The single-beat method for estimating the EDPVR is somewhat simpler, requiring only measurement of end-diastolic and pressure coordinates (V_{ed}, P_{ed}; Figure 3F).[20] Based upon the observation that when normalized to volume, the shape of the EDPVR stays constant, this method has been validated using ex vivo and in vivo LV PV data (12).

CLINICAL APPLICATIONS FOR RV PV ANALYSIS

With improved catheter technology and easier signal processing, RV PV analysis is being performed with increased regularity in several clinical scenarios (Figure 4). In these scenarios, patients typically undergo noninvasive evaluations of RV function with multiple different modalities (ie, echocardiography and cross-sectional imaging) which yield conflicting conclusions or are incongruent with their symptomatology. PV analysis can help resolve the uncertainty created by these noninvasive studies by quantifying RV systolic and diastolic function and the nature of ventricular-vascular interactions with measures like the RV-PA coupling ratio. Additionally, PV analysis can be used in clinical contexts where characterizing immediate changes in RV function during an intervention is useful (ie, LVAD speed optimization test or transcatheter edge-to-edge tricuspid repair). Below, we review some of these applications and illustrate how RV PV analysis can provide a comprehensive picture of RV performance which is ultimately clinically relevant and impactful for diagnosis, management, and prognostication.

Resting and Exertional RV Function in the Healthy Heart

Cornwell et al[21] performed the first-in-human RV PV analysis in healthy subjects during rest and exercise in an upright position. In so doing, they demonstrated the feasibility of PV loop acquisition during upright cycle ergometry. PV loops from these healthy individuals displayed the classic domed shape and illustrate how RV end-systolic pressure decays nearly to end-diastolic pressure during exercise and, unlike LV physiology, that ejection proceeds well past end-systole. The loops illustrate that the healthy

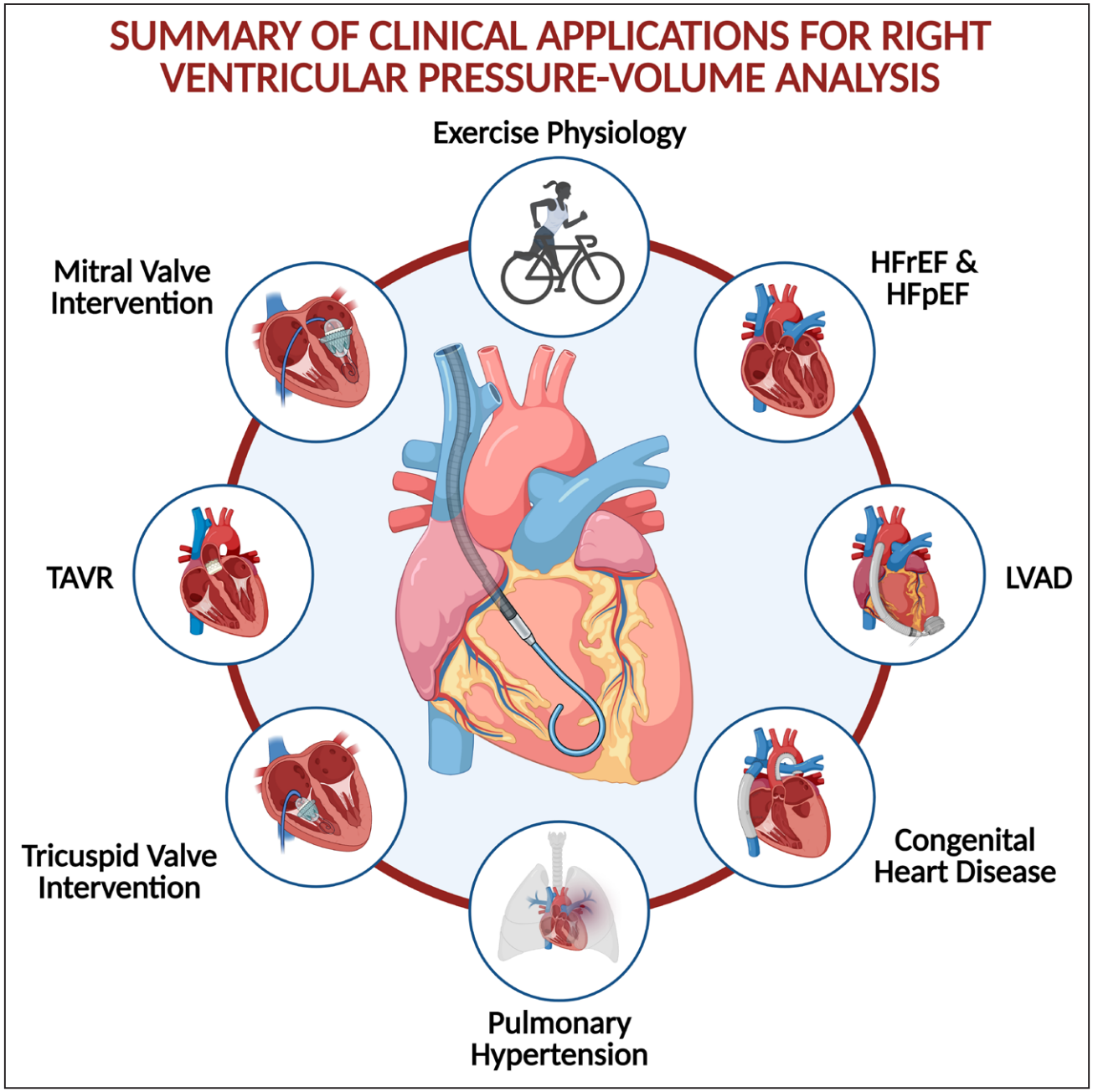

Figure 4. Summary of clinical applications for right ventricular (RV) pressure-volume analysis.
RV pressure-volume analysis can help characterize RV physiology in a variety of conditions and clinical settings. HFpEF indicates heart failure preserved ejection fraction; HFrEF, heart failure reduced ejection fraction; LVAD, left ventricular assist device; and TAVR, transcatheter aortic valve replacement.

RV is a highly compliant chamber with a large contractile reserve; indices of contractility increase by 3- to 4-fold from rest to peak exercise (Figure S3).[22] RV-PA coupling (indexed by the ratio between E_{es} and E_a)[23] was also maintained throughout the spectrum of exercise intensity as E_{es} increased in step with the rise of E_a.[24]

Pulmonary Hypertension

The ability to simultaneously describe ventricular and vascular properties makes PV analysis a valuable tool to characterize the hemodynamic consequences of pulmonary hypertension. For example, in World Health Organization Group I PAH, where RV function strongly influences prognosis, PV analysis is helpful in identifying early stages of RV systolic dysfunction that would otherwise go unrecognized by traditional imaging and hemodynamics modalities. RV diastolic stiffness, when assessed by properties of the EDPVR, is also associated with disease progression in patients with PAH.[25] The PV loop in PAH, where PA pressures approach systemic pressures, morphs and can take on a distinctive,

notched, or trapezoidal shape (Figure 5).[26] Specifically in this setting, Hsu[27] also demonstrated that RV-PA coupling, assessed by the ratio of E_{es} to E_a, identified occult RV dysfunction with greater sensitivity than traditional measures. More than just an academic construct, catheter-derived E_{es}/E_a predicted clinical worsening in patients with PAH better than existing measures like RV ejection fraction (EF), suggesting that such measurements can add value to current standards of practice.[28] In addition, Tedford et al[29] found that E_{es}/E_a identified RV dysfunction which was not even detected during RHC.[29] At a mechanistic level, derangements in RV E_{es} correlate with intrinsic RV myocyte dysfunction, providing a plausible explanation for the association with adverse outcomes.[30]

Heart Failure With Preserved Ejection Fraction

Heart failure with preserved ejection fraction (HFpEF) has now outpaced HF with reduced EF as the leading cause of HF.[31] HFpEF is associated with a poor prognosis, especially in patients with concurrent RV dysfunction, which occurs in up to half of all HFpEF cases.[32,33] PV analysis may help resolve some of the significant knowledge gaps that remain regarding the underlying pathophysiology of HFpEF and the RV's contribution to the pathophysiology in many well-recognized HFpEF populations. PV analysis may also facilitate deeper understanding of the different HFpEF phenotypes and predict response to various treatments.

To this end, Rommel et al[34] performed the first-in-human RV PV analysis in patients with HFpEF. Patients with HFpEF had preserved RV systolic function with E_{es} values that were higher than in healthy controls but demonstrated severe impairments in diastolic function such as increased load-independent RV stiffness and impaired active relaxation, akin to what has been previously documented in the LV of patients with HFpEF (Figure S4). These abnormalities were even more pronounced with stress and handgrip exercise, where the RV was unable to increase SV and augment cardiac output.

A more recent study pairing PV analysis with CMR suggested more wide-ranging abnormalities in the right heart in patients with HFpEF and implicated an abnormal interplay between the right atrium and RV (ie, RA-RV coupling) as an important contributor to the pathophysiology of HFpEF.[35] This observation may be a hallmark of early adaptations to HFpEF physiology in the RA-RV-PA circuit which eventually progresses over time and evolves into the combined systolic and diastolic RV dysfunction observed in later stages of HFpEF.[36] Considering the prevalence of HFpEF and the many unanswered questions regarding the pathophysiology, PV analysis is

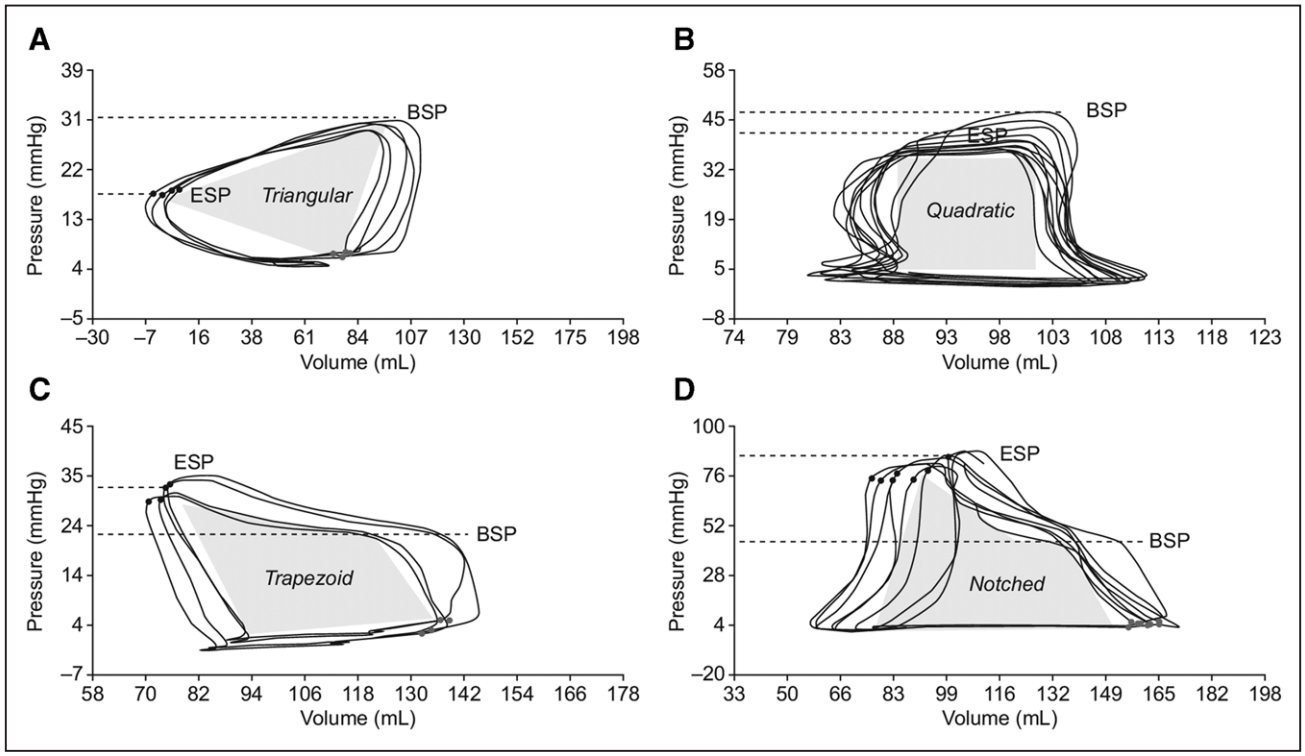

Figure 5. Changes in the right ventricular (RV) pressure-volume (PV) loop contour in patients with versus without pulmonary hypertension.

Characteristic triangular (**A**), quadratic (**B**), trapezoid (**C**), and notched (**D**) RV PV loop morphologies, which are associated with varying differentials between pulmonary artery (PA) beginning systolic pressure (BSP) and end-systolic pressure (ESP). Adapted from Richter et al[26] with permission. Copyright ©2021, The American Physiological Society.

primed to play an important role in future studies seeking to further characterize the hemodynamic perturbations associated with HFpEF, the determinants of disease progression, and response to different therapies.

Durable Mechanical Circulatory Support

RV function influences symptoms, quality of life, and prognosis for patients with end-stage HF supported by a LVAD. While invasive evaluations of RV function (ie, RHC-guided hemodynamic-echocardiographic speed optimization tests) may optimize LVAD performance,[37] our understanding, at a mechanistic level, of the nature of RV dysfunction post-LVAD implantation is limited. A recently published study applying RV PV analysis to LVAD recipients demonstrated that even patients with echocardiographically normal appearing RVs had only modest inotropic reserve during exercise and experienced dramatically increased LV filling pressures.[38] Another analysis demonstrated changes in systolic and diastolic function with increasing LVAD speed, lending credence to the theory that at least in some patients, LV unloading may contribute to RV dysfunction due to interventricular interactions (Figure 6).[39] In this study, 3 different patterns of interventricular interaction were observed as a function of LVAD speed: cases with changes in RV diastolic function only, changes in RV diastolic and systolic function, and cases without any changes in the RV PV loop with increased LVAD speed. The RV became more compliant with increased LVAD speed, indicating favorable effects on diastolic function, while contractility tended to decline, suggesting unfavorable effects on systolic function. The balance between these opposing forces is patient specific and further work is required to determine the prevalence of these different RV responses to LV unloading and their clinical implications.

Furthermore, PV analysis may also ultimately help address 2 critical, clinically relevant questions in patients with end-stage HF with reduced EF with durable mechanical support: (1) what LVAD speed optimizes LV function, aortic valve opening while minimizing aortic insufficiency, septal position, and reduces mitral regurgitation and (2) which patients benefit from upfront RV mechanical circulatory support at the time of LVAD implantation. The ongoing REVIVAL-VAD trial (Right Heart Catheterization and Pressure Volume Analysis in the Right Ventricle in Patients Before and After Left Ventricular Assist Device Implantation) aims to resolve these areas of uncertainty and will be an important proof-of-concept study for using PV analysis in a clinical context.

Valvular Heart Disease

Finally, the burgeoning field of transcatheter therapy for valvular heart disease presents a unique opportunity to evaluate RV physiology with PV analysis. Despite satisfactory clinical outcomes in randomized controlled trials of interventions for aortic stenosis, there is broad variability in outcomes in real-world practice following technically successful transcatheter aortic valve replacement and surgical aortic valve replacement, which may be explained by preprocedural and postprocedural RV dysfunction.[40] To date, there is only one report describing RV PV loops in a patient with bicuspid aortic valve disease and severe aortic stenosis.[5] The RV loops featured a prominent isovolumic contraction phase, similar to what is observed with LV PV loops, suggesting the presence of increased afterload in the pulmonary circulation, akin to what has been described in conditions like PAH (Figure 7A). The LV PV loops during transcatheter aortic valve replacement deployment with a balloon expandable valve show signs of significant ventricular stunning following the period of rapid pacing and valve deployment and only partial recovery by the end of the procedure, raising concerns that a similar phenomenon may occur in the RV, where the capacity to recover may be even more limited.

Atrioventricular valve disease presents an even more interesting opportunity for RV PV analysis given the strong interaction between mitral regurgitation or TR and RV function. Prognosis for patients with primary mitral regurgitation, for example, is worse with concomitant RV dysfunction,[41] and patients fare worse after transcatheter edge-to-edge repair if RV dysfunction persists postprocedure.[42] Our group was the first to document changes to the RV PV loop in this setting.[43] We showed that V-wave reduction and decreased left atrial pressure following transcatheter edge-to-edge repair resulted in a significant decline in RV E_a, implicating the role of downstream pressure in RV afterload (Figure 7B). Further research is required to characterize the RV PV loop in different forms of mitral regurgitation (ie, primary versus secondary) and how it responds to different interventions such as transcatheter edge-to-edge repair or transcatheter mitral valve replacement.

The tricuspid valve is arguably the most enigmatic of all heart valves. The surge of novel catheter-based tricuspid valve repair techniques offers new perspectives for the treatment of severe TR.[44] Timing of such TR intervention and periprocedural evaluation of TR reduction maneuvers are critical to determine procedural success and predict short- and long-term clinical outcomes. As such, PV analysis can guide TR reduction treatment by monitoring RV contractility, loading, and RV-PA coupling preprocedure and postprocedure; benefits which are all the more relevant considering the well-established limitations of echocardiographic assessments in the setting of severe TR.[45] Figure 7C is a case-in-point illustration of how PV analysis clarifies the physiological effects of transcatheter edge-to-edge tricuspid repair. Ventricular unloading occurs with an acute reduction in end-diastolic volume as SV declines but is accompanied by an increase

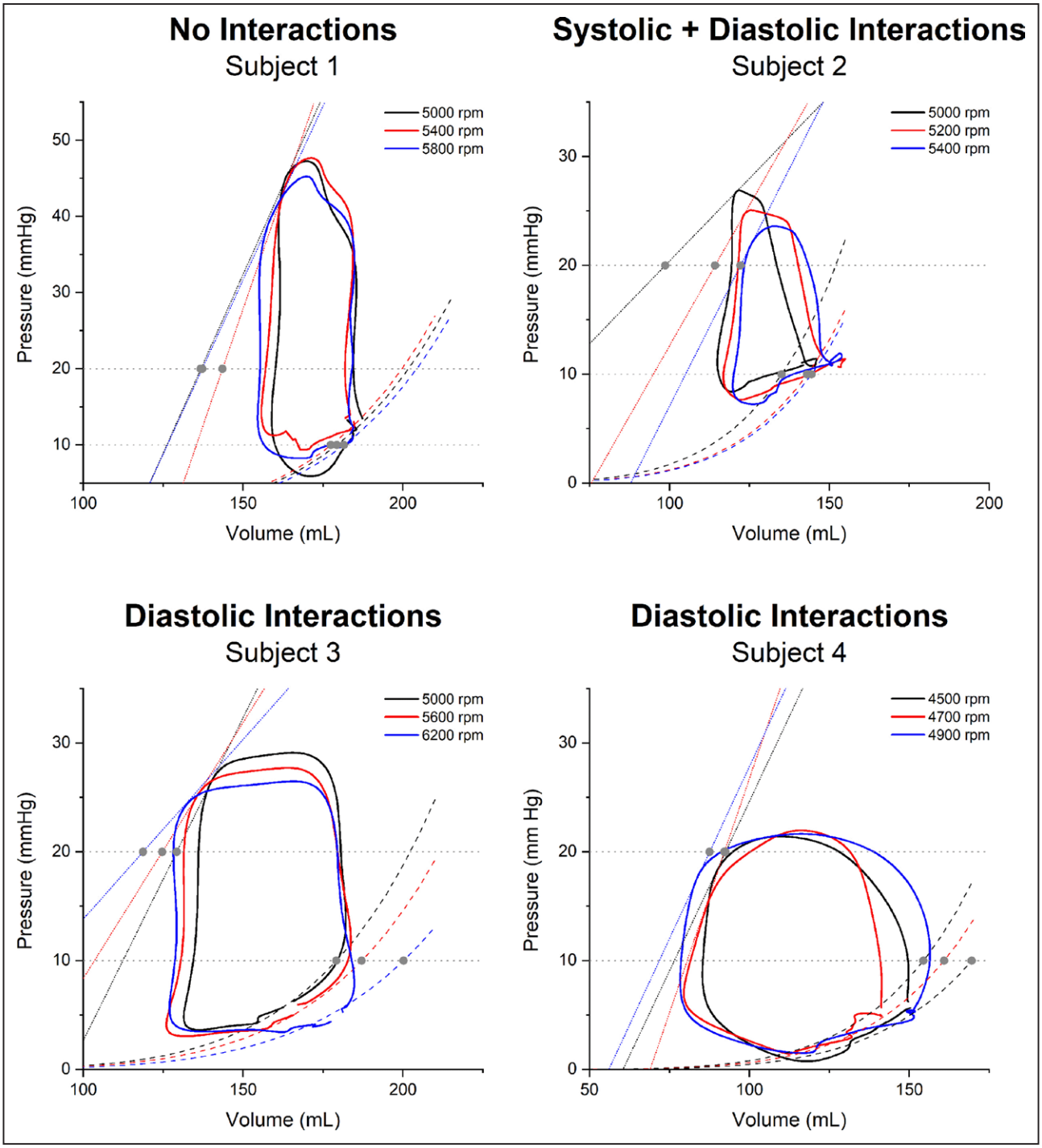

Figure 6. Changes in right ventricular properties with increasing left ventricular assist device speed.
Changes in systolic and diastolic function result in decreased contractile function and increased ventricular compliance, respectively. These changes were not reproduced uniformly in a series of 4 patients during a left ventricular assist device speed optimization test. Adapted from Brener et al[39] with permission. Copyright ©2021, Elsevier.

in afterload as blood is diverted from the low-pressure atrial environment into the higher resistance environment of the PA. This increase in afterload may explain the clinical deterioration observed in some patients, particularly those with advanced RV dysfunction, in response to transcatheter edge-to-edge tricuspid repair or other tricuspid valve interventions.

PV ANALYSIS WITHOUT A CONDUCTANCE CATHETER

PV loop acquisition, as detailed in the sections above, is inherently invasive. Hence, there is substantial interest in reconstructing PV loops using data obtained noninvasively or with routinely collected data from

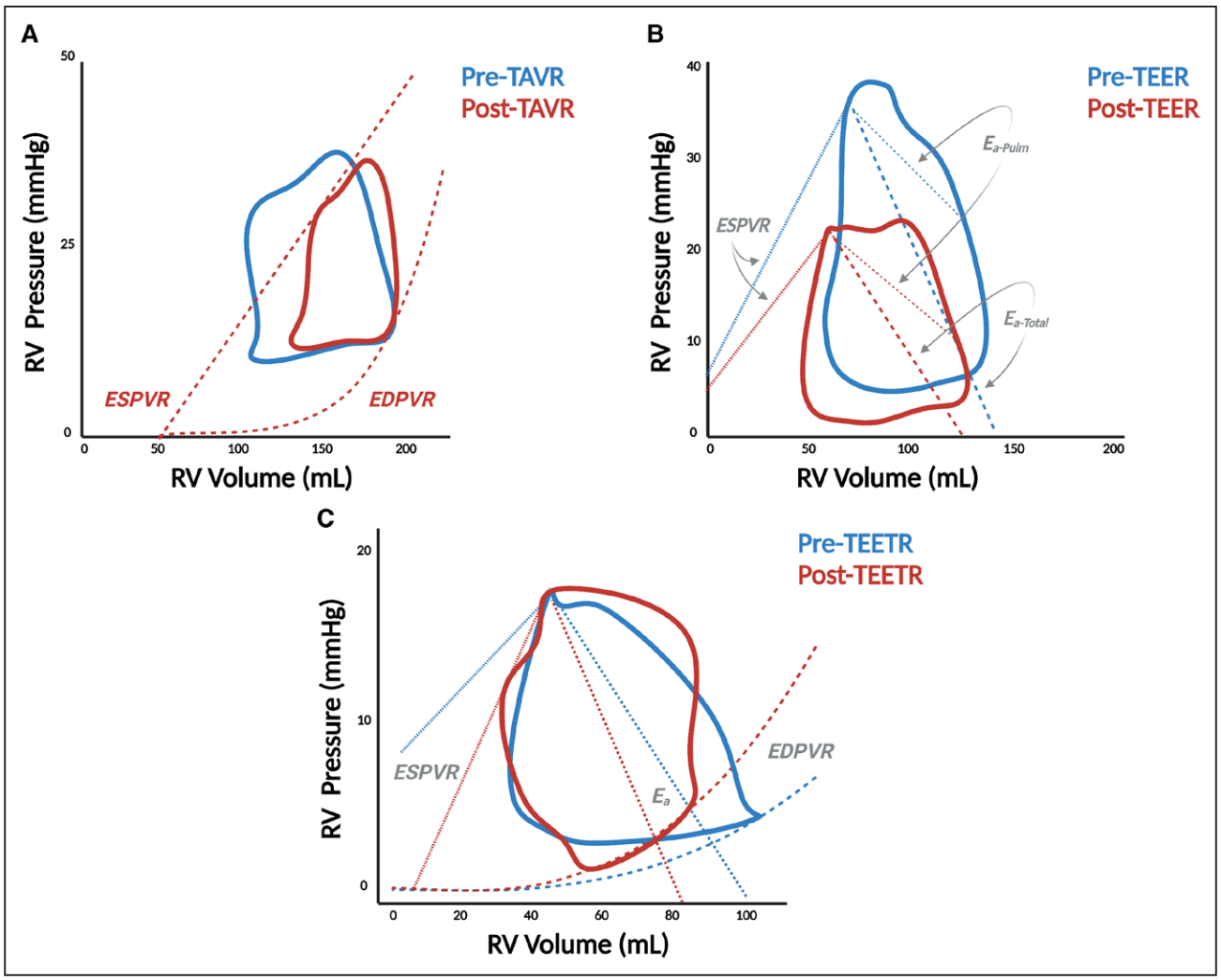

Figure 7. Right ventricular (RV) pressure-volume (PV) loops before and after transcatheter valvular intervention.
PV analysis demonstrates significant changes in RV physiology before and after transcatheter aortic valve replacement (TAVR; **A**), as well as transcatheter edge-to-edge repair (TEER) in the mitral (**B**) and tricuspid (TEETR; **C**) positions. E_a indicates effective arterial elastance; EDPVR, end-diastolic PV relationship; E_{es}, end-systolic elastance; and ESPVR, end-systolic PV relationship.

standard-of-care procedures like RHC (Figure 8). This is particularly relevant in the context of well-described limitations correlating conductance catheter measurements with echocardiographic surrogates (ie, r=0.356 for tricuspid annular systolic plane excursion and RV E_{es}).[46] To this end, over the last decade, CMR has been used to reconstruct elements of the PV loop and, in particular, estimate RV-PA coupling.[47,48] While the ECG can be used to synchronize separately measured CMR derived volumes and RV pressure waveforms to reconstruct PV loops, the most accurate method requires simultaneous RHC and cine MRI, which is challenging to perform outside of research settings.[49]

More recently, Richter et al[50] recently validated a method recreating RV PV loops by synchronizing volume-time curves (V(*t*)) from 3-dimensional echocardiography and pressure-time curves (P(*t*)) generated by either directly measured RV pressure using a pressure wire in the ventricle or echocardiographic measurements of RV pressure aligned with specific events during the cardiac cycle (ie, pulmonic valve opening).[50] This latter, echocardiography-based technique has been corroborated in the LV and performed acceptably against invasive RV PV loops.[51] Echocardiography-based estimates of E_{es} and E_{es}/E_a coupling were highly correlated with conductance catheter-based measurements (ρ=0.8053 and 0.8261, respectively), but this method did not perform particularly well in capturing energetic measurements like stroke work (Figure 1; the area within the PV loop). This technique relies on a reference pressure-time curve, constructed by averaging pressure tracings from multiple individuals and may only be valid for specific pathologies because the nature of RV pressure generation varies depending on the underlying disease and patient substrate. The method also relies on excellent acoustic windows to produce accurate volume-time curves, which may be particularly challenging in patients with a history of prior open-heart surgery (ie, LVAD recipients).

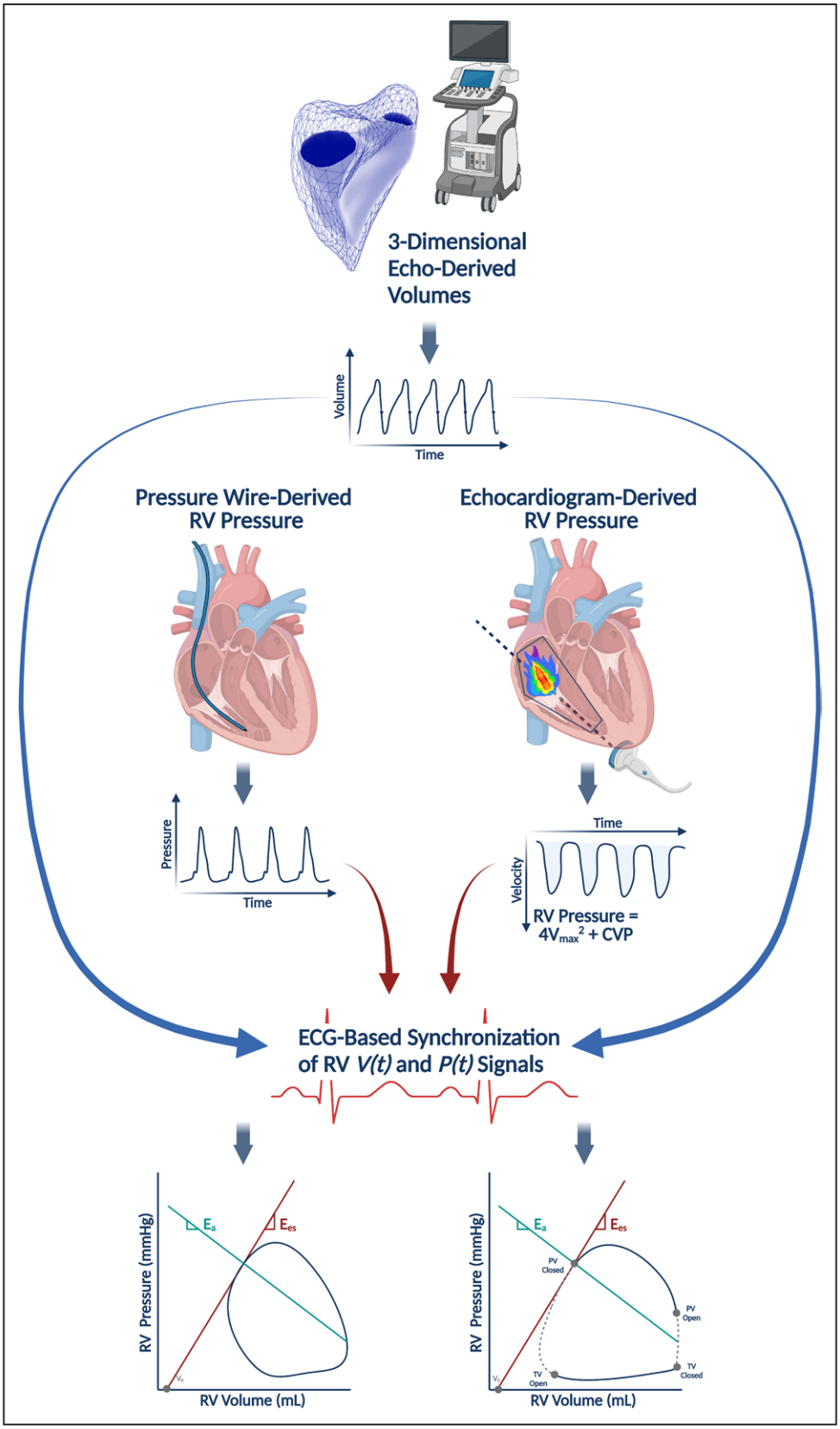

Figure 8. Noninvasive derivation of right ventricular (RV) pressure-volume (PV) loops.
PV loops can be reconstructed without a conductance catheter by synchronizing a volume-time signal (V(*t*)) from 3-dimensional echocardiography with a pressure-time signal (P(*t*)). The pressure-time signal can be obtained with a pressure wire in the RV or noninvasively estimated from echocardiograms by measuring the RV systolic pressure from a tricuspid regurgitant jet. Adapted from Richter et al[50] with permission. Copyright ©2021, Oxford University Press.

Further work is needed to assess whether this framework can be replicated in larger cohorts (including patients without pulmonary hypertension), to build reference pressure-time and volume-time curve libraries, and to understand under what particular conditions the necessary assumptions for this technique to be applied are violated. Moreover, this method needs to outperform other noninvasive indices to justify routine use (ie, tricuspid annular systolic plane excursion/PA systolic pressure, a noninvasive surrogate of RV-PA coupling that is associated with outcomes in patients with mitral regurgitation,[52] TR,[53] and HF with reduced[54] or preserved[55] EF despite modest correlation with RV E_{es}/E_a measured with a conductance catheter [r=0.71][46]). These limitations notwithstanding, the potential of noninvasive PV loop assessment is significant: by easing the barriers to data acquisition, noninvasive PV loops may become a fast, convenient way to monitor changes in ventricular function over time or in response to certain interventions.

CONCLUSIONS

PV analysis is a potent platform for describing RV physiology in health and disease. Considered the gold-standard method for quantifying intrinsic chamber systolic and diastolic properties, it has a powerful role in diagnosis and prognostication in various RV disease states, especially as providers become more comfortable using conductance catheters and interest in invasive hemodynamic assessment grows. Having highlighted all that can be gleaned from RV PV analysis based on invasive conductance catheter measurements, it is critical that investigators are aware of its limitations. The calibration technique is challenging, and analysis and interpretation of the loops still involves making certain assumptions or subjective decisions. Therefore, it is vitally important that PV loop acquisition and analysis be standardized, and investigators adopt uniform reporting practices as the technique is more widely adopted and incorporated into various research and clinical practices.

ARTICLE INFORMATION

Affiliations

Division of Cardiology, Columbia University Medical Center, New York, NY (M.I.B., A.M., V.G.N., R.T.H., S.K.K., G.T.S., N.U., D.B.). Cardiovascular Research Foundation, New York, NY (D.B.). Department of Internal Medicine, Justus Liebig Universitat Giessen, Germany (K.T.). Department of Interventional Cardiology, Thoraxcenter, Erasmus University Medical Center, Rotterdam, the Netherlands (M.B.B., A.J.M.V.D.E., N.M.V.M.). Division of Cardiology, University of Colorado Anschutz Medical Campus, Aurora (W.K.C.). Division of Cardiology, Johns Hopkins University School of Medicine, Baltimore, MD (S.H.). Division of Cardiology, Medical University of South Carolina, Charleston (R.J.T.). Division of Cardiology, Heart Center, University of Leipzig, Germany (P.L., K.-P.R., K.-P.K.). Section of Cardiology, Houston Methodist DeBakey Heart and Vascular Center, TX (S.F.N.). Cardiovascular Institute, Alleghany Health Network, Pittsburgh, PA (M.K.K.). Cardiovascular Center and Molecular Cardiology Research Institute, Tufts Medical Center, Boston, MA (N.K.K.). Division of Pediatric Cardiology, University of Minnesota Masonic Children's Hospital, Minneapolis (G.H.). Division of Cardiology, Mayo Clinic, Rochester, MN (M.S.). Division of Anesthesiology, Yale University School of Medicine, New Haven, CT (P.M.H.).

Acknowledgments

The authors thank Patrick Sullivan for his assistance. Figures were created with BioRender.com.

Sources of Funding

Dr Brener is supported by the National Heart, Lung, and Blood Institute (T32HL007343) and the American College of Cardiology/Merck Research Fellowship.

Disclosures

Dr Tello has received speaking fees from Actelion and Bayer. Dr Bastos receives personal fees from PulseCath BV. Dr Cornwell reports consulting fees and research funding from Medtronic. Dr Tedford reports no direct conflicts of interest related to this article but notes the following general disclosures: consulting relationships with Medtronic, Abbott, Aria CV Inc, Acceleron, Itamar, Edwards LifeSciences, Eidos Therapeutics, Lexicon Pharmaceuticals, Gradient, and United Therapeutics. Dr Hsu is on a steering committee for Medtronic, Acceleron, and Abbott, as well as a research advisory board for Abiomed, and also does hemodynamic core lab work for Actelion and Merck. Dr Kanwar is on the Abiomed advisory board. Dr Van Mieghem reports research grant support from Abbott Vascular, Boston Scientific, Medtronic, Edwards Lifesciences, PulseCAth BV, Abiomed, and Daiichi Sankyo. Dr Hiremath is a consultant for Abbott, B.Braun, Merit, and KA Medical. Dr Kapur reports institutional research grants and speaker/consulting honoraria from Abbott, Abiomed, Boston Scientific, Getinge, Medtronic, LivaNova, MDStart, preCARDIA, and Zoll. Dr Hahn has served as a consultant for Abbott Vascular, Abbott Structural, NaviGate, Philips Healthcare, Medtronic, Edwards Lifesciences, and GE Healthcare; is the Chief Scientific Officer for the Echocardiography Core Laboratory at the Cardiovascular Research Foundation for multiple industry-supported trials, for which she receives no direct industry compensation; has received speaker fees from Boston Scientific and Baylis Medical; and has received nonfinancial support from 3mensio. Dr Kodali has served on the scientific advisory board for Microinterventional Devices, Dura Biotech, Thubrikar Aortic Valve, and Supira; has served as a consultant for Meril Lifesciences, Admedus, Medtronic, and Boston Scientific; has served on the steering committee for Edwards Lifesciences and Abbott Vascular; has received honoraria from Meril Lifesciences, Admedus, Abbott Vascular, and Dura Biotech; and owns equity in Dura Biotech, Thubrikar Aortic Valve, Supira, and MID. Dr Sayer reports consulting fees from Abbott. Dr Uriel reports consulting fees from Medtronic and has received honorarium from Abbott. Dr Burkhoff discloses consulting fees from PVLoops and Cardiodyme and has received grant support from Abiomed. The other authors report no conflicts.

Supplemental Material

Figures S1–S4

REFERENCES

1. Sanz J, Sánchez-Quintana D, Bossone E, Bogaard HJ, Naeije R. Anatomy, function, and dysfunction of the right ventricle: JACC state-of-the-art review. *J Am Coll Cardiol*. 2019;73:1463–1482. doi: 10.1016/j.jacc.2018.12.076
2. Brener MI, Burkhoff D, Sunagawa K. Effective arterial elastance in the pulmonary arterial circulation: derivation, assumptions, and clinical applications. *Circ Heart Fail*. 2020;13:e006591. doi: 10.1161/CIRCHEARTFAILURE.119.006591
3. Vonk-Noordegraaf A, Westerhof N. Describing right ventricular function. *Eur Respir J*. 2013;41:1419–1423. doi: 10.1183/09031936.00160712
4. Bastos MB, Burkhoff D, Maly J, Daemen J, den Uil CA, Ameloot K, Lenzen M, Mahfoud F, Zijlstra F, Schreuder JJ, et al. Invasive left ventricle pressure-volume analysis: overview and practical clinical implications. *Eur Heart J*. 2020;41:1286–1297. doi: 10.1093/eurheartj/ehz552
5. Sarraf M, Burkhoff D, Brener MI. First-in-man 4-chamber pressure–volume analysis during transcatheter aortic valve replacement for bicuspid aortic valve disease. *JACC Case Rep*. 2021;3:77–81. doi: 10.1016/j.jaccas.2020.11.041
6. Brener MI, Burkhoff D, Basir MB, Alqarqaz M. Pressure-volume analysis illustrating the mechanisms of short-term hemodynamic effects produced by premature ventricular contractions. *Circ Heart Fail*. 2021;14:e007766. doi: 10.1161/CIRCHEARTFAILURE.120.007766

7. Burkhoff D. The conductance method of left ventricular volume estimation. Methodologic limitations put into perspective. *Circulation*. 1990;81:703–706. doi: 10.1161/01.cir.81.2.703
8. Baan J, van der Velde ET, de Bruin HG, Smeenk GJ, Koops J, van Dijk AD, Temmerman D, Senden J, Buis B. Continuous measurement of left ventricular volume in animals and humans by conductance catheter. *Circulation*. 1984;70:812–823. doi: 10.1161/01.cir.70.5.812
9. Maughan WL, Shoukas AA, Sagawa K, Weisfeldt ML. Instantaneous pressure-volume relationship of the canine right ventricle. *Circ Res*. 1979;44:309–315. doi: 10.1161/01.res.44.3.309
10. Ten Brinke EA, Burkhoff D, Klautz RJ, Tschöpe C, Schalij MJ, Bax JJ, van der Wall EE, Dion RA, Steendijk P. Single-beat estimation of the left ventricular end-diastolic pressure-volume relationship in patients with heart failure. *Heart*. 2010;96:213–219. doi: 10.1136/hrt.2009.176248
11. ten Brinke EA, Klautz RJ, Verwey HF, van der Wall EE, Dion RA, Steendijk P. Single-beat estimation of the left ventricular end-systolic pressure-volume relationship in patients with heart failure. *Acta Physiol (Oxf)*. 2010;198:37–46. doi: 10.1111/j.1748-1716.2009.02040.x
12. Sunagawa K, Yamada A, Senda Y, Kikuchi Y, Nakamura M, Shibahara T, Nose Y. Estimation of the hydromotive source pressure from ejecting beats of the left ventricle. *IEEE Trans Biomed Eng*. 1980;27:299–305. doi: 10.1109/TBME.1980.326737
13. Brimioulle S, Wauthy P, Ewalenko P, Rondelet B, Vermeulen F, Kerbaul F, Naeije R. Single-beat estimation of right ventricular end-systolic pressure-volume relationship. *Am J Physiol Heart Circ Physiol*. 2003;284:H1625–H1630. doi: 10.1152/ajpheart.01023.2002
14. Senzaki H, Chen CH, Kass DA. Single-beat estimation of end-systolic pressure-volume relation in humans. A new method with the potential for noninvasive application. *Circulation*. 1996;94:2497–2506. doi: 10.1161/01.cir.94.10.2497
15. Trip P, Kind T, van de Veerdonk MC, Marcus JT, de Man FS, Westerhof N, Vonk-Noordegraaf A. Accurate assessment of load-independent right ventricular systolic function in patients with pulmonary hypertension. *J Heart Lung Transplant*. 2013;32:50–55. doi: 10.1016/j.healun.2012.09.022
16. Bellofiore A, Vanderpool R, Brewis MJ, Peacock AJ, Chesler NC. A novel single-beat approach to assess right ventricular systolic function. *J Appl Physiol (1985)*. 2018;124:283–290. doi: 10.1152/japplphysiol.00258.2017
17. Tello K, Richter MJ, Axmann J, Buhmann M, Seeger W, Naeije R, Ghofrani HA, Gall H. More on single-beat estimation of right ventriculoarterial coupling in pulmonary arterial hypertension. *Am J Respir Crit Care Med*. 2018;198:816–818. doi: 10.1164/rccm.201802-0283LE
18. Heerdt PM, Kheyfets V, Charania S, Elassal A, Singh I. A pressure-based single beat method for estimation of right ventricular ejection fraction: proof of concept. *Eur Respir J*. 2020;55:1901635. doi: 10.1183/13993003.01635-2019
19. Richter MJ, Peters D, Ghofrani HA, Naeije R, Roller F, Sommer N, Gall H, Grimminger F, Seeger W, Tello K. Evaluation and prognostic relevance of right ventricular-arterial coupling in pulmonary hypertension. *Am J Respir Crit Care Med*. 2020;201:116–119. doi: 10.1164/rccm.201906-1195LE
20. Rain S, Handoko ML, Trip P, Gan CT, Westerhof N, Stienen GJ, Paulus WJ, Ottenheijm CA, Marcus JT, Dorfmüller P, et al. Right ventricular diastolic impairment in patients with pulmonary arterial hypertension. *Circulation*. 2013;128:2016–25, 1. doi: 10.1161/CIRCULATIONAHA.113.001873
21. Cornwell WK, Coe G, Ambardekar A, Pal J, Tompkins C, Zipse M, Wolfel G, Brieke A, Levine B, Kohrt W. Abstract 13179: new insights into right ventricular performance during exercise using high-fidelity conductance catheters to generate pressure volume loops. *Circulation*. 2018;138:A13179–A13179.
22. Walker LA, Buttrick PM. The right ventricle: biologic insights and response to disease: updated. *Curr Cardiol Rev*. 2013;9:73–81. doi: 10.2174/1573403X13805076296
23. Tello K, Gall H, Richter M, Ghofrani A, Schermuly R. Right ventricular function in pulmonary (arterial) hypertension. *Herz*. 2019;44:509–516. doi: 10.1007/s00059-019-4815-6
24. Cornwell WK, Tran T, Cerbin L, Coe G, Muralidhar A, Hunter K, Altman N, Ambardekar AV, Tompkins C, Zipse M, et al. New insights into resting and exertional right ventricular performance in the healthy heart through real-time pressure-volume analysis. *J Physiol*. 2020;598:2575–2587. doi: 10.1113/JP279759
25. Trip P, Rain S, Handoko ML, van der Bruggen C, Bogaard HJ, Marcus JT, Boonstra A, Westerhof N, Vonk-Noordegraaf A, de Man FS. Clinical relevance of right ventricular diastolic stiffness in pulmonary hypertension. *Eur Respir J*. 2015;45:1603–1612. doi: 10.1183/09031936.00156714
26. Richter MJ, Hsu S, Yogeswaran A, Husain-Syed F, Vadász I, Ghofrani HA, Naeije R, Harth S, Grimminger F, Seeger W, et al. Right ventricular pressure-volume loop shape and systolic pressure change in pulmonary hypertension. *Am J Physiol Lung Cell Mol Physiol*. 2021;320:L715–L725. doi: 10.1152/ajplung.00583.2020
27. Hsu S. Coupling right ventricular-pulmonary arterial research to the pulmonary hypertension patient bedside. *Circ Heart Fail*. 2019;12:e005715. doi: 10.1161/CIRCHEARTFAILURE.118.005715
28. Hsu S, Simpson CE, Houston BA, Wand A, Sato T, Kolb TM, Mathai SC, Kass DA, Hassoun PM, Damico RL, et al. Multi-beat right ventricular-arterial coupling predicts clinical worsening in pulmonary arterial hypertension. *J Am Heart Assoc*. 2020;9:e016031. doi: 10.1161/JAHA.119.016031
29. Tedford RJ, Mudd JO, Girgis RE, Mathai SC, Zaiman AL, Housten-Harris T, Boyce D, Kelemen BW, Bacher AC, Shah AA, et al. Right ventricular dysfunction in systemic sclerosis-associated pulmonary arterial hypertension. *Circ Heart Fail*. 2013;6:953–963. doi: 10.1161/CIRCHEARTFAILURE.112.000008
30. Hsu S, Kokkonen-Simon KM, Kirk JA, Kolb TM, Damico RL, Mathai SC, Mukherjee M, Shah AA, Wigley FM, Margulies KB, et al. Right ventricular myofilament functional differences in humans with systemic sclerosis-associated versus idiopathic pulmonary arterial hypertension. *Circulation*. 2018;137:2360–2370. doi: 10.1161/CIRCULATIONAHA.117.033147
31. van Riet EE, Hoes AW, Wagenaar KP, Limburg A, Landman MA, Rutten FH. Epidemiology of heart failure: the prevalence of heart failure and ventricular dysfunction in older adults over time. A systematic review. *Eur J Heart Fail*. 2016;18:242–252. doi: 10.1002/ejhf.483
32. Gorter TM, van Veldhuisen DJ, Bauersachs J, Borlaug BA, Celutkiene J, Coats AJS, Crespo-Leiro MG, Guazzi M, Harjola VP, Heymans S, et al. Right heart dysfunction and failure in heart failure with preserved ejection fraction: mechanisms and management. Position statement on behalf of the Heart Failure Association of the European Society of Cardiology. *Eur J Heart Fail*. 2018;20:16–37. doi: 10.1002/ejhf.1029
33. Melenovsky V, Hwang SJ, Lin G, Redfield MM, Borlaug BA. Right heart dysfunction in heart failure with preserved ejection fraction. *Eur Heart J*. 2014;35:3452–3462. doi: 10.1093/eurheartj/ehu193
34. Rommel KP, von Roeder M, Oberueck C, Latuscynski K, Besler C, Blazek S, Stiermaier T, Fengler K, Adams V, Sandri M, et al. Load-independent systolic and diastolic right ventricular function in heart failure with preserved ejection fraction as assessed by resting and handgrip exercise pressure-volume loops. *Circ Heart Fail*. 2018;11:e004121. doi: 10.1161/CIRCHEARTFAILURE.117.004121
35. von Roeder M, Kowallick JT, Rommel KP, Blazek S, Besler C, Fengler K, Lotz J, Hasenfuß G, Lücke C, Gutberlet M, et al. Right atrial-right ventricular coupling in heart failure with preserved ejection fraction. *Clin Res Cardiol*. 2020;109:54–66. doi: 10.1007/s00392-019-01484-0
36. Borlaug BA, Kane GC, Melenovsky V, Olson TP. Abnormal right ventricular-pulmonary artery coupling with exercise in heart failure with preserved ejection fraction. *Eur Heart J*. 2016;37:3293–3302. doi: 10.1093/eurheartj/ehw241
37. Uriel N, Sayer G, Addetia K, Fedson S, Kim GH, Rodgers D, Kruse E, Collins K, Adatya S, Sarswat N, et al. Hemodynamic ramp tests in patients with left ventricular assist devices. *JACC Heart Fail*. 2016;4:208–217. doi: 10.1016/j.jchf.2015.10.001
38. Tran T, Muralidhar A, Hunter K, Buchanan C, Coe G, Hieda M, Tompkins C, Zipse M, Spotts MJ, Laing SG, et al. Right ventricular function and cardiopulmonary performance among patients with heart failure supported by durable mechanical circulatory support devices. *J Heart Lung Transplant*. 2021;40:128–137. doi: 10.1016/j.healun.2020.11.009
39. Brener MI, Hamid NB, Fried JA, Masoumi A, Raikhelkar J, Kanwar MK, Pahuja M, Mondellini GM, Braghieri L, Majure DT, et al. Right ventricular pressure-volume analysis during left ventricular assist device speed optimization studies: insights into interventricular interactions and right ventricular failure. *J Card Fail*. 2021;27:991–1001. doi: 10.1016/j.cardfail.2021.04.019
40. Généreux P, Pibarot P, Redfors B, Mack MJ, Makkar RR, Jaber WA, Svensson LG, Kapadia S, Tuzcu EM, Thourani VH, et al. Staging classification of aortic stenosis based on the extent of cardiac damage. *Eur Heart J*. 2017;38:3351–3358. doi: 10.1093/eurheartj/ehx381
41. Le Tourneau T, Deswarte G, Lamblin N, Foucher-Hossein C, Fayad G, Richardson M, Polge AS, Vannesson C, Topilsky Y, Juthier F, et al. Right ventricular systolic function in organic mitral regurgitation: impact of biventricular impairment. *Circulation*. 2013;127:1597–1608. doi: 10.1161/CIRCULATIONAHA.112.000999
42. Ledwoch J, Fellner C, Hoppmann P, Thalmann R, Kossmann H, Dommasch M, Dirschinger R, Stundl A, Laugwitz KL, Kupatt C. Impact of transcatheter mitral valve repair using MitraClip on right ventricular remodeling. *Int J Cardiovasc Imaging*. 2020;36:811–819. doi: 10.1007/s10554-020-01771-2

43. Brener MI, Burkhoff D, Sarraf M. Right ventricular pressure-volume analysis before and after transcatheter leaflet approximation for severe mitral regurgitation. *JAMA Cardiol*. 2021;6:e207209. doi: 10.1001/jamacardio.2020.7209
44. Taramasso M, Benfari G, van der Bijl P, Alessandrini H, Attinger-Toller A, Biasco L, Lurz P, Braun D, Brochet E, Connelly KA, et al. Transcatheter versus medical treatment of patients with symptomatic severe tricuspid regurgitation. *J Am Coll Cardiol*. 2019;74:2998–3008. doi: 10.1016/j.jacc.2019.09.028
45. Hahn RT, Zamorano JL. The need for a new tricuspid regurgitation grading scheme. *Eur Heart J Cardiovasc Imaging*. 2017;18:1342–1343. doi: 10.1093/ehjci/jex139
46. Schmeisser A, Rauwolf T, Groscheck T, Kropf S, Luani B, Tanev I, Hansen M, Meißler S, Steendijk P, Braun-Dullaeus RC. Pressure–volume loop validation of TAPSE/PASP for right ventricular arterial coupling in heart failure with pulmonary hypertension. *Eur Heart J Cardiovasc Imaging*. 2020;22:168–176.
47. Breeman KTN, Dufva M, Ploegstra MJ, Kheyfets V, Willems TP, Wigger J, Hunter KS, Ivy DD, Berger RMF, Truong U. Right ventricular-vascular coupling ratio in pediatric pulmonary arterial hypertension: a comparison between cardiac magnetic resonance and right heart catheterization measurements. *Int J Cardiol*. 2019;293:211–217. doi: 10.1016/j.ijcard.2019.05.021
48. Sanz J, García-Alvarez A, Fernández-Friera L, Nair A, Mirelis JG, Sawit ST, Pinney S, Fuster V. Right ventriculo-arterial coupling in pulmonary hypertension: a magnetic resonance study. *Heart*. 2012;98:238–243. doi: 10.1136/heartjnl-2011-300462
49. Kuehne T, Yilmaz S, Steendijk P, Moore P, Groenink M, Saaed M, Weber O, Higgins CB, Ewert P, Fleck E, et al. Magnetic resonance imaging analysis of right ventricular pressure-volume loops: in vivo validation and clinical application in patients with pulmonary hypertension. *Circulation*. 2004;110:2010–2016. doi: 10.1161/01.CIR.0000143138.02493.DD
50. Richter MJ, Yogeswaran A, Husain-Syed F, Vadász I, Rako Z, Mohajerani E, Ghofrani HA, Naeije R, Seeger W, Herberg U, et al. A novel non-invasive and echocardiography-derived method for quantification of right ventricular pressure–volume loops. *Eur Heart J Cardiovasc Imaging*. 2021. jeab038. doi: 10.1093/ehjci/jeab038
51. Russell K, Eriksen M, Aaberge L, Wilhelmsen N, Skulstad H, Remme EW, Haugaa KH, Opdahl A, Fjeld JG, Gjesdal O, et al. A novel clinical method for quantification of regional left ventricular pressure-strain loop area: a non-invasive index of myocardial work. *Eur Heart J*. 2012;33:724–733. doi: 10.1093/eurheartj/ehs016
52. Karam N, Stolz L, Orban M, Deseive S, Praz F, Kalbacher D, Westermann D, Braun D, Näbauer M, Neuss M, et al. Impact of right ventricular dysfunction on outcomes after transcatheter edge-to-edge repair for secondary mitral regurgitation. *JACC Cardiovasc Imaging*. 2021;14:768–778. doi: 10.1016/j.jcmg.2020.12.015
53. Fortuni F, Butcher SC, Dietz MF, van der Bijl P, Prihadi EA, De Ferrari GM, Ajmone Marsan N, Bax JJ, Delgado V. Right ventricular-pulmonary arterial coupling in secondary tricuspid regurgitation. *Am J Cardiol*. 2021;148:138–145. doi: 10.1016/j.amjcard.2021.02.037
54. Bosch L, Lam CSP, Gong L, Chan SP, Sim D, Yeo D, Jaufeerally F, Leong KTG, Ong HY, Ng TP, et al. Right ventricular dysfunction in left-sided heart failure with preserved versus reduced ejection fraction. *Eur J Heart Fail*. 2017;19:1664–1671. doi: 10.1002/ejhf.873
55. Guazzi M, Dixon D, Labate V, Beussink-Nelson L, Bandera F, Cuttica MJ, Shah SJ. RV contractile function and its coupling to pulmonary circulation in heart failure with preserved ejection fraction: stratification of clinical phenotypes and outcomes. *JACC Cardiovasc Imaging*. 2017;10(10 pt B):1211–1221. doi: 10.1016/j.jcmg.2016.12.024